Research Article

BIOMEDICAL Journal of Scientific & Technical Research

ISSN: 2574 -1241

DOI: 10.26717/BJSTR.2023.53.008474

# Preparation of $Cu^{I}Y$ from Binary $Cu^{II}$ Precursors and its CO Adsorption Performance

**Xue Li[1], Jiali Zhang[1,2]*, Dapeng Li[1], Can Zhu[1,2] and Yulong Zhang[1,2]***

[1]*College of Chemistry and Chemical Engineering, Henan Polytechnic University, PR China*

[2]*Henan Key Laboratory of Coal Green Conversion, Henan Polytechnic University, PR China*

***Corresponding author:** Jiali Zhang and Yulong Zhang, College of Chemistry and Chemical Engineering, Henan Key Laboratory of Coal Green Conversion, Henan Polytechnic University, Jiaozuo, Henan 454000, PR China

**ARTICLE INFO**

**Received:** November 20, 2023

**Published:** November 29, 2023

**Citation:** Xue Li, Jiali Zhang, Dapeng Li, Can Zhu and Yulong Zhang. Preparation of $Cu^{I}Y$ from Binary $Cu^{II}$ Precursors and its CO Adsorption Performance. Biomed J Sci & Tech Res 53(5)-2023. BJSTR. MS.ID.008474.

**ABSTRACT**

Separation and purification of CO is an important chemical process. Adsorption is competitive due to its efficient operation, low energy and mature technology. For CO adsorption, the capacity and selectivity of the adsorbent is the key factor to determine the efficiency. In this paper, alcohol was used as the dispersing agent, and $CuCl_2$ and $Cu(CH_3COO)_2$ were used as the precursors mixing with HY molecular sieve, then followed by activation at different temperatures to prepare CO adsorbents. The maximum CO adsorption capacity was 42 mL $g^{-1}$, which was 28.4 % higher than that of the adsorbent prepared with water as the dispersing agent. The adsorbents were characterized by BET, XRD, XRF, XPS and TG-MS. It was revealed that $Cu^{II}$ can be reduced to $Cu^{I}$ at 290°C and highly dispersed on surface of HY. Ion exchange occurred between HY molecular sieve and $Cu^{I}$ salts, and $Cu^{I}Y$ came into being. Compared with $Cu^{II}$, $Cu^{0}$ and even CuY/HY, $Cu^{I}Y$ had the best CO adsorption performance.

**Keywords:** $Cu^{I}Y$; Binary $Cu^{II}$ Precursors; Solvent; CO adsorption

## Introduction

Carbon Monoxide (CO) is well known as an important chemical raw material. The synthesis of carbon-based chemicals such as acetic acid, dimethyl carbonate, acetic anhydride, methyl format and isocyanate all require high-purity CO as the raw materials [1-3]. CO is a toxic air pollutant that has brought up environmental problems such as acid rain, ozone depletion and climate change, which can lead to significant health risk [4,5]. Moreover, slight CO is a harmful substance in some industrial gas, which can deactivate the active sites of catalyst, especially for some precious metal catalysts such as Pt et al. [6,7] Therefore, the separation and purification of CO from gas mixtures is necessary due to its industrial benefits and environmental effects. There are many methods to separate CO from mixed gases such as cryogenic distillation, absorption and adsorption [8-10]. In theory, separation is an energy-consuming process because the second law of thermodynamics does not favor it. Compared with the traditional technologies, adsorption is competitive due to its low energy cost, efficient operation and matured technology [11,12]. In adsorption separation, the commonly used carriers are molecular sieve, activated carbon, synthetic resin, activated alumina and other porous carriers [13-15]. Molecular sieve has been widely considered as a promising adsorbent material for CO separation and purification due to its good thermal stability, excellent adsorption selectivity, large specific surface area and narrow pore size distribution [16,17]. For CO adsorption, the capacity and selectivity of the adsorbent is the key factor to determine the efficiency. Many adsorbents incorporated by $Cu^{I}$ or $Ag^{I}$ have received much attention because they can capture CO molecules through π-complexation [18,19]. Compared with physical adsorption, the π-complexation bonds are generally stronger than electrostatic

and Van der Waals interactions, so it shows higher selectivity. Compared with general chemisorption, its relative weak π-complexation force make it easy to regenerate [19]. In particular, $Cu^{I}$ adsorbent, due to its cheap and easy availability, is regarded as a promising adsorbent, has been widely studied in recent years.

Traditionally, adsorbent was made by single copper precursors. As early as the 1970s, the United Carbon Corporation (UCC, US) had reported a patent about CO adsorbent prepared by ion exchange of $Cu^{+}$ or $Ag^{+}$, but its CO adsorption performance was poor [20]. Based on a general principle that compounds tend to spontaneously disperse on the high surface supports to form a monolayer, Xie et al. prepared $CuCl/Y$ adsorbent by a thermal treatment of a mixture of $CuCl$ and Y molecular sieve [17,21]. The results showed that $CuCl$ dispersed uniformly on Y molecular sieve at atomic level and the adsorbent was widely used in industry [22]. Takahashi et al. exchanged excess $Cu(NO_3)_2$ solution with $NaY$ for 24 hours at room temperature and reduced $Cu^{2+}$ to $Cu^{+}$ using different reducing agents such as ammonia or CO, followed by activation at 300-450 ℃ under He [23]. Sun et al. used $NaY$ molecular sieve as carrier and $CuCl_2$ as precursor and prepared $CuCl/Y$ under mild reduction of glucose. It was found that the separation performance and the stability of the absorbent were good. The application of single copper precursor was restricted due to their instability or insolubility. In order to introduce more $Cu^{I}$ on molecular sieve, multiple attempts have been made. Using binary $Cu^{II}$ precursors was a potential solution to solve the problems such as low-loading and easy oxidation. Some researchers had already made some explorations [5]. A $CuCl/AC$ adsorbent was made by a facile route of physically mixing $CuCl_2$ and $Cu(HCOO)_2$ powder with Activated Carbon (AC), followed by heating at 533 K under vacuum, and the result was good. It is well known that $CuCl_2$ and $Cu(CH_3COO)_2$ are more stable and cheaper than $CuCl$ and $Cu(HCOO)_2$, and HY molecular sieve has higher thermal stability than active carbon. In this paper, CO adsorbent was prepared using binary $Cu^{II}$ precursors and different dispersing agents, and the carrier was HY molecular sieve.

## Experimental

### Materials and Preparations

$CuCl_2{\cdot}2H_2O$ was obtained from Tianjin Fengchuan Chemical Co., Ltd.(Tianjin city, China), $Cu(CH_3COO)_2{\cdot}H_2O$ and $C_2H_5OH$ were purchased from Tianjin Hongyan Chemical Co., Ltd.( Tianjin city, China ), and they were all AR grade without further purification. HY molecular sieve ($SiO_2/A1_2O_3$ = 5.4) was purchased from Tianjin Nankai Catalyst Factory (Tianjin city, China), which was pretreated before use. CO and Ar (99.999 %) were obtained from Henan Yuanzheng Special Gas Ltd. (Xinxiang city, China), $N_2$ (99.999 %) was purchased from Henan Ruian Keji Co. Ltd. (Zhengzhou city, China), as listed in Table 1. $Cu^{I}/Y$ were prepared from binary $Cu^{II}$ precursors using different dispersing agents. Firstly, different mole ratio of $Cu(CH_3COO)_2{\cdot}H_2O/CuCl_2{\cdot}2H_2O$ (the total amount of $Cu^{2+}$ was certain) were dissolved in a solvent (deionized water or $C_2H_5OH$). Secondly, the pretreated HY was added to the above solution, and the hydrothermal ion exchange was performed at different temperature for 12 h. Thirdly, The sediment was separated via centrifugation. Finally, the sediment was dried and activated in a tube furnace under Ar flow. The experiments were conducted by heating the sediments from room temperature to the final temperatures at a rate of 2ºC $min^{-1}$, followed by an isothermal treatment for 4 h and finally cooled down to room temperature.

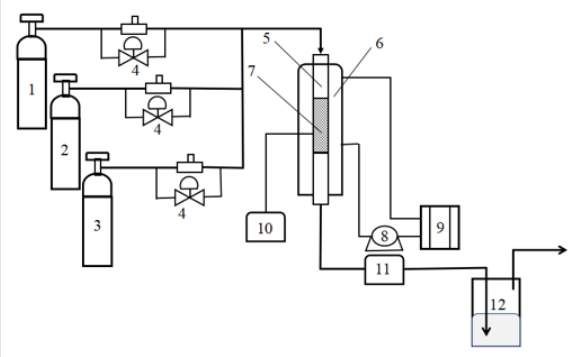


Note: 1. $N_2$; 2. 1% CO; 3. $H_2$; 4. Mass flowmeter; 5. Quartz tube; 6. Tubular furnace; 7. Adsorbent; 8. Pump; 9. Low temperature circulation tank; 10. Temperature controller; 11. Gas analyzer; 12. Tail gas absorption

**Figure 1:** Schematic diagram of CO adsorption/desorption.

### CO Adsorption/Regeneration Measurements

Dynamic adsorption of CO was evaluated with a fixed bed, as shown in Figure 1 (Jiaozuo city, China). 1 g tablet sample was put into a quartz tube with a diameter of 10 mm and a length of 38 mm. The adsorption temperature was maintained at 30ºC by a electric furnace temperature controller and a cryogenic coolant circulation tank. The $N_2$ flow containing 1 % CO passed through the fixed bed at a flow rate of 150 mL $min^{-1}$. The adsorbed gas was detected by KE200-U multi-component gas analyzer (Xi'an Kepeng Electrical Equipment Co., Ltd. Xian city, China) with an accuracy of 1 ppm and a range of 0-1000 ppm. In the breakthrough experiment, the zero-time was determined by the blank test. The breakthrough point was set at the concentration of each adsorbent in outlet gas reached 5 % of the component in the feed. The tail gas was vented to the atmosphere after absorption. Regeneration was performed with $N_2$ as the regeneration gas. The relative experimental error of the estimated amounts was lower than ± 5 %.

### CO Adsorption Isothermal

The adsorption isotherms of CO were measured by a corrosive gas adsorption analyzer BSD-PMC (Beishide Instrument, Beijing city, China). Approximately 0.1 g of the sample was degassed at 523 K for 3 h in vacuum. The adsorption capacity of the adsorbent were obtained by a static volumetric method at 30°C with a error of ± 1 %.

### Characterization

The crystalline structures of $Cu^{I}Y$ adsorbents were examined by powder X-ray diffractometer (EMPYREAN, Holland). The X-ray diffractometer used Cu Kα radiation. The tube voltage and current were 40 kV and 30 mA, respectively. For all samples, the 2θ angle was scanned from 5° to 60° with a scanning speed of 5° $min^{-1}$ and 0.02° per step. The XRD patterns were analyzed using MDI Jade software package. Nitrogen adsorption-desorption isotherms (BET) were obtained at -196 K using ASAP-2460 instrument. The samples were outgassed at 250°C for 3 h in a dynamic vacuum before the adsorption isotherm was determined. The PSD was obtained from Density Functional Theory (DFT) method. The total pore volume ($V_t$) was generated according to the $N_2$ adsorption at the relative pressure (P/P0) of 0.99. Micropore volume ($V_{mic}$), Micropore volume ($V_{mic}$), micropore ratio surface ($S_{mic}$) and external surface area ($S_{ex}$) were obtained by the t-plot method.

### XRF Experiments

The main elemental components of the prepared adsorbents was tested by X-ray Fluorescence Spectroscopy (XRF). In this paper, Thermo Scientific ARL Perform'X X-ray fluorescence spectrometer was used to test the powder adsorbents.

### XPS experiments

The chemical state of copper in CO adsorbents were investigated by X-ray photoelectron spectrometer (XPS). XPS analysis were performed by XSAM800 instrument from KRATOS, UK. With Al Kα monochromatic radiation (1486.6 eV) and a high-vacuum chamber, the anode was operated at 120 W, and the analyzer was operated at a constant narrow scan pass energy of 30 eV. The XPS analysis was calibrated by the C1s peak at 284.6 eV. Due to the coexistence of $Cu^{I}$ and $Cu^{II}$, the XPS spectra were deconvoluted using the casa XPS software and the peak position and peak region were determined.

### TG-MS Experiments

In order to explore the mechanism of adsorbent in preparation, the Thermogravimetric and Mass Spectrometric Experiments (TG-MS) were conducted on NETZSCH STA449F3-QMS403 Aeolos Quadro analyzer coupled with a mass spectrometer. About 14 mg of un-activated sample were placed in a ceramic crucible. The samples were heated from room temperature to 290 °C with a heating rate of 5 °C $min^{-1}$ followed by an isothermal period for 1 h. The experiments used high purity Ar as carrier gas at a constant flow rate of 50 mL $min^{-1}$.

## Results and Discussion

### CO Adsorption

Figure 2 showed CO adsorption breakthrough capacities of the prepared adsorbents. According to the literature, [17,21], [24-26] the dispersion of copper in HY molecular sieve was a key factor affecting CO adsorption. Figure 2a summarized the effect of solvent in solvothermal process on adsorbent performance. When using water as the solvent, the CO adsorption breakthrough capacity of the prepared adsorbents were 1.14 mL $g^{-1}$, 9.87 mL $g^{-1}$ and 4.79 mL $g^{-1}$ respectively. However, when using $C_2H_5OH$ as the solvent, the CO adsorption breakthrough capacity of the prepared adsorbents significantly improved, which were 1.35 mL $g^{-1}$, 10.00 mL $g^{-1}$ and 12.67 mL $g^{-1}$ respectively. The CO adsorption breakthrough capacity of the adsorbent prepared with $C_2H_5OH$ as solvent was 28.4 % higher than that of the adsorbent prepared with water as the solvent. It indicated that, in solvothermal process, the solvent played an important role in ion exchange and ion distribution. Different solvent had different solubility, polarity, surface tension and volatility, which resulted in a different presence state and mobility of copper salts in solvothermal process. $C_2H_5OH$ is a good dispersing agent in chemical industry. When $C_2H_5OH$ was used as the solvent, it would enhance the mass transfer and distribution of the copper salts in $HY$ molecular sieve.

 **DOI:** 10.26717/BJSTR.2023.53.008474

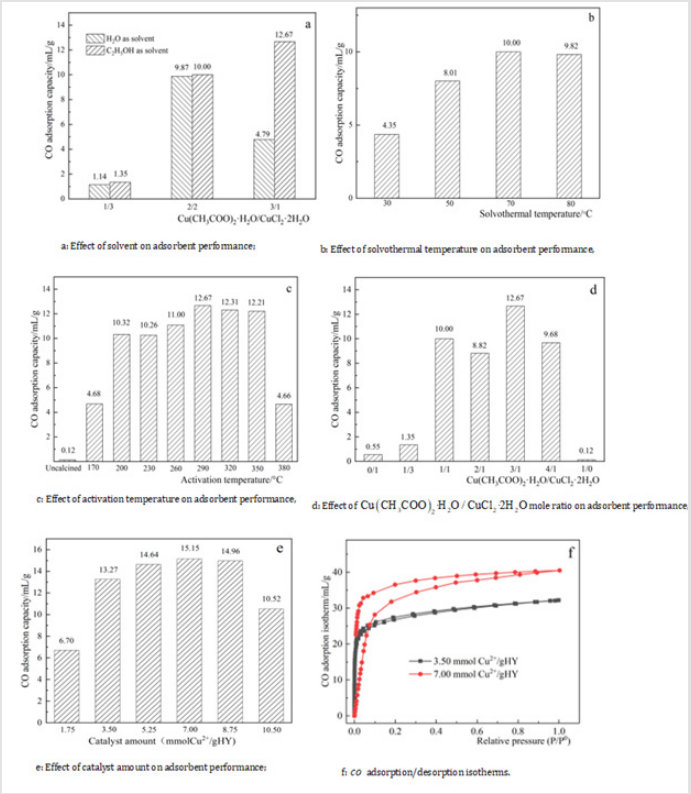


**Figure 2:** *co* adsorption of prepared adsorbents.

So, $C_2H_5OH$ was chosen as the solvent in solvothermal process in this paper. Figure 2b showed the effect of solvothermal temperature on adsorbent performance. In solvothermal process, with increasing solvothermal temperature, the thermal motion of the ions in solution became more active, which enhanced the mass transfer and ion exchange in solvothermal process. Therefore, high solvothermal temperature was beneficial to improve the CO adsorption performance of the adsorbent. Considering the volatility of the solvent, 70 ℃ was chosen as the solvothermal temperature. Figure 2c showed the effect of activation temperature on adsorbent performance. Before activation, the adsorbent had a very low CO adsorption capacity, as listed in Figure 2c. According to the literature, $Cu^{II}$ almost had no contribution to CO adsorption [27-29]. $Cu^{I}$ was recognized as the preferred adsorbent form, which had appropriate affinity to CO in CO adsorption. In order to change the valence state of copper from $Cu^{2+}$ to $Cu^{+}$, it was necessary to activate the sediments. The activation temperature directly affected the adsorbent performance because it determined the amount of $Cu^{I}$ active sites generated. With the increase of activation temperature, the CO adsorption capacity of the prepared adsorbents increased obviously. When the activation temperature was 290 ℃, the CO adsorption capacity of the adsorbent reached the highest, indicating more $Cu^{I}$ active sites generated. When the activation temperature increased further, the CO adsorption capacity of the adsorbent did not increase, but decreased gradually. The reason may exist in two aspects: one was that higher temperature turned $Cu^{I}$ into $Cu^{0}$, which had low CO adsorption ability; The other was that higher temperature may cause the aggregation of the active sites [30-32]. So, the activation temperature was chosen as 290 ℃.

It was important to choose an appropriate $CuCl_2 \cdot 2H_2O / Cu(CH_3COO)_2 \cdot H_2O$ mole ratio. Figure 2d showed the effect of $Cu(CH_3COO)_2 \cdot H_2O / CuCl_2 \cdot 2H_2O$ mole ratio on adsorbent performance. Even if the total amount of copper was constant, the CO adsorption capacity of the adsorbents were quite different. Whether water or $C_2H_5OH$ as the solvent, it was obvious that the prepared adsorbent had a very low CO adsorption capacity when using a single $Cu(CH_3COO)_2$ or $CuCl_2$ as the copper precursor. The reasons were as follows: 1) Very little $Cu^{2+}$ loading onto HY molecular sieve through ion exchange; 2) Very little amount of $Cu^{2+}$ converted into $Cu^{+}$ during activation process. More explorations were needed. With binary copper salts as the precursors, the experimental results were interesting. As listed in Figure 2a, when using water as the solvent, the optimal mole

ratio of $Cu(CH_3COO)_2 \cdot H_2O / CuCl_2 \cdot 2H_2O$ was 1/1. Xue had revealed the mechanism of equal mole of $Cu(HCOO)_2$ and $CuCl_2$ impregnating on the surface of the active carbon: [5]

$$Cu(HCOO)_2 + CuCl_2 = 2CuCl + H_2O + CO_2 + CO \quad (1)$$

The divalent copper was reduced to monovalent copper via self-redox reactions, and the monovalent copper was highly dispersed on the surface of AC. When the mole ratio of $Cu(HCOO)_2 / CuCl_2$ was small, the decomposition product $Cu(HCOO)_2$ was not enough to reduce $CuCl_2$ to monovalent copper, resulting in less active sites on the adsorbent, so the CO adsorption capacity was small; When the mole ratio of $Cu(HCOO)_2 / CuCl_2$ was 1, $Cu(HCOO)_2$ was appropriate to reduce $CuCl_2$ to monovalent copper, resulting in much active sites on the adsorbent, so the CO adsorption capacity was large; When the molar ratio of $Cu(HCOO)_2 / CuCl_2$ was greater than 1, a part of $Cu(HCOO)_2$ reduced $CuCl_2$ to monovalent copper, producing the active site, and another pare of $Cu(HCOO)_2$ played a small role in CO adsorption, so the CO adsorption capacity was reduced, as shown in (1).

While using $C_2H_5OH$ as the solvent, the experiment results were different. As listed in Figure 2a, when the mole ratio of $Cu(CH_3COO)_2 \cdot H_2O / CuCl_2 \cdot 2H_2O$ was 1/3, the CO adsorption capacity was only 1.35 mL $g^{-1}$. When the mole ratio of $Cu(CH_3COO)_2 \cdot H_2O / CuCl_2 \cdot 2H_2O$ was 1/1, the CO adsorption capacity of the prepared adsorbent increased significantly, which was similar to that of the adsorbent prepared with water as the solvent. When the mole ratio of $Cu(CH_3COO)_2 \cdot H_2O / CuCl_2 \cdot 2H_2O$ was 3/1, the CO adsorption breakthrough capacity of the prepared adsorbent reached a maximum, which was 12.67 mL $g^{-1}$. It was strange that the optimal mole ratio of $Cu(CH_3COO)_2 \cdot H_2O / CuCl_2 \cdot 2H_2O$ was no longer 1/1, but 3/1. The experimental results indicated that, more complicated mechanism perhaps occurred. $C_2H_5OH$ probably acted not only as a dispersion agent, but also as a reducing agent in the interaction. In the similar self-redox reactions described above, $C_2H_5OH$ also played a role, resulting in the presence of more active $Cu^I$ in the adsorbent and further exploration was needed. In summary, the optimal mole ratio of $Cu(CH_3COO)_2 \cdot H_2O / CuCl_2 \cdot 2H_2O$ was chosen as 3/1.

The total copper amount was also important because it decided the number of $Cu^I$ active sites in HY molecular sieve. The $Cu(CH_3COO)_2 \cdot H_2O / CuCl_2 \cdot 2H_2O$ mole ratio was fixed at 3/1, and the effect of total copper amount on adsorbent performance was illustrated in Figure 2e. The results showed that, as the total copper amount increased from 1.75 mmol $Cu^{2+}(gHY)^{-1}$ to 7.0 mmol $Cu^{2+}(gHY)^{-1}$, the CO breakthrough adsorption capacity increased from 6.70 mL $g^{-1}$ to 15.15 mL $g^{-1}$. However, it gradually decreased with the further increase of the total copper amount. Adsorption occurs at the active sites of the adsorbent. At low copper loading, optimal CO adsorption capacity may not be reached due to lack of active sites, while excess copper loading may block the pore entrances of the HY molecular sieve to decrease the surface area and CO adsorption capacity. Therefore, the optimal copper loading was 7.00 mmol $Cu^{2+}(gHY)^{-1}$.

An adsorption isotherm can provide information on the adsorption capacity of an adsorbents. Figure 2f illustrated the CO adsorption/desorption isotherms. It was a typical type I isotherm, suggesting the strong interaction between CO and the adsorbent via a π-complexation. In the plateau for the adsorbent (7.0 mmol $Cu^{2+}(gHY)^{-1}$ ) was reached at 42 mL $g^{-1}$. While for the adsorbent (3.5 mmol $Cu^{2+}(gHY)^{-1}$, the plateau was reached at about 30 mL $g^{-1}$. That was, the adsorbent with 7.0 mmol $Cu^{2+}(gHY)^{-1}$ contributed more active sites than the adsorbent with 3.5 mmol $Cu^{2+}(gHY)^{-1}$. The stability of CuY was tested in the fixed bed. The regeneration was performed at 100 °C at atmospheric pressure at $N_2$ flow rate of 100 mL $min^{-1}$. After 5 times of adsorption and regeneration, the adsorption capacity was almost unchanged, indicating that the character of the adsorbents were stable.

**Adsorbents Characterization**

Figures 3a & 3b illustrated the $N_2$ adsorption-desorption equilibrium isotherms (BET) of HY molecular sieve and the adsorbents prepared with different amount of copper loading at 77 K. According to IUPAC, the adsorption-desorption isotherms of $N_2$ all exhibited the typical type I isotherm that was obtained on micro-porous materials, where mono-layers adsorption were formed on the surface [33,34]. From Figure 3a, it was found that, with the increase of copper loading on the adsorbents, their $N_2$ adsorption amounts apparently decreased. The BET surface area, pore volume and average pore diameters of HY molecular sieve and the adsorbents prepared with different amount of copper loading were summarized in Table 2. With the copper loading increasing, the specific surface area and pore volume of the molecular sieve decreased gradually because the copper loaded on the cage of the HY molecular sieve. For the typical type I isotherm, the surface area of the sample was much smaller than the surface area of the hole volume, and the adsorption capacity was controlled by the volume of the hole. As for the CO adsorption, the adsorption of CO was not only closely related to its specific surface area, but also to the amount of active sites. For the copper loading on the molecular sieve, on the one hand, it increased the number of CO adsorption active sites, but on the other hand, it reduced the specific surface area of the molecular sieve. This conclusion was consistent with the experimental results, as shown in Table 1. It could be observed that the CO adsorption capacity increased from 0.12 mL $g^{-1}$ to 15.15 mL $g^{-1}$ with the increase of copper loading amount from 0 to 7.0 mmol $Cu^{2+}(gHY)^{-1}$, which was attributed to the π complexation between CO and $Cu^I$ active sites of the adsorbents. The CO adsorption/desorption

isotherms of the adsorbents were in good agreement with the figure of $N_2$ adsorption-desorption isotherms, indicating that all the micropores were all accessible to CO. When the copper loading amount increased from 7.0 mmol $Cu^{2+}(gHY)^{-1}$ to 10.5 mmol $Cu^{2+}(gHY)^{-1}$, the CO adsorption capacity decreased slightly because much copper active site reduced the specific area of the Y molecular sieve.

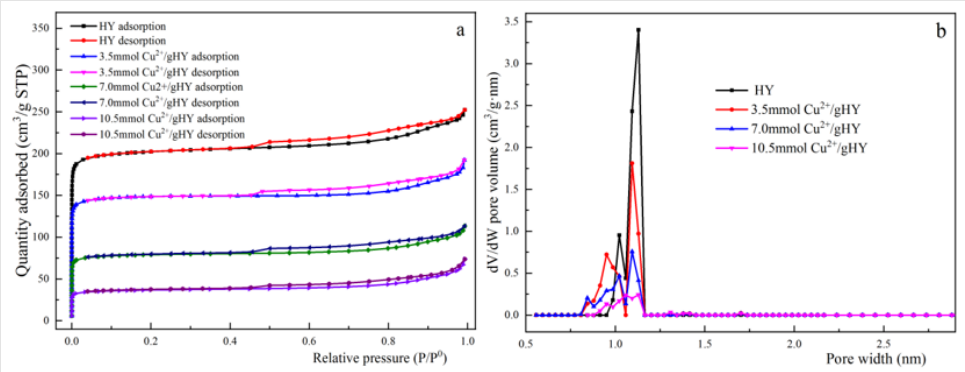


**Figure 3:** $N_2$ adsorption-desorption equilibrium isotherms of HY molecular sieve and the adsorbents prepared with different amounts of copper loadings.

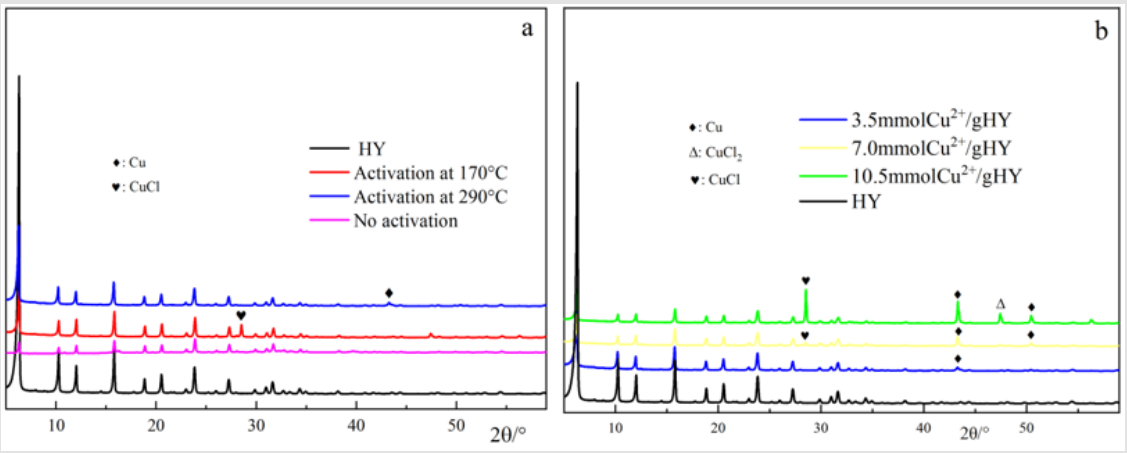


**Figure 4:** XRD patterns of HY molecular sieve and prepared adsorbents.

**Table 1:** CAS registry number, purity, and analysis method of the chemicals.

| Component | CAS Reg, No. | Suppliers | Purity (%) | Analysis method |
|---|---|---|---|---|
| HY molecular sieve | 69912-79-4 | Tianjin Nankai Catalyst Factory | | |
| $Cu(CH_3COO)_2 \cdot H_2O$ | 6046-93-1 | Tianjin Hongyan Chemical Co., Ltd. | AR | AAS |
| $CuCl_2 \cdot 2H_2O$ | 10125-13-0 | Tianjin Fengchuan Chemical Co., Ltd. | AR | AAS |
| $C_2H_5OH$ | 64-17-5 | Tianjin Hongyan Chemical Co., Ltd. | AR | GC |
| CO | 630-08-0 | Henan Yuanzheng Special Gas Ltd. | 99.999 | IR |

| | | | | |
|---|---|---|---|---|
| $N_2$ | 7727-37-9 | Henan Ruian Keji Co., Ltd. | 99.999 | IR |
| Ar | 7440-37-1 | Henan Yuanzheng Special Gas Ltd. | 99.999 | IR |

**Table 2:** Physical adsorption parameters of adsorbents at different activation temperatures.

| Adsorbent | $a_{s,BET}$ ($m^2 \cdot g^{-1}$) | $V_{total}$ ($P/P_0$=0.99) ($cm^3/g$) | Average pore diamerter (nm) | CO adsorption capacity (mL/g) |
|---|---|---|---|---|
| HY | 819 | 0.39 | 1.905 | 0.12 |
| 3.5mmol $Cu^{2+}$/gHY | 606 | 0.298 | 1.964 | 12.42 |
| 7.0 mmol $Cu^{2+}$/gHY | 318 | 0.176 | 2.21 | 15.15 |
| 10.5 mmol $Cu^{2+}$/gHY | 145 | 0.114 | 3.136 | 10.52 |

Figure 4a illustrated the XRD patterns of HY molecular sieve and the adsorbents activated at different temperatures. Compared with HY molecular sieve, the crystalline structure of the adsorbents were well maintained after activated at different temperatures [35]. Before activation, though there were $Cu(CH_3COO)_2 \cdot H_2O$ and $CuCl_2 \cdot 2H_2O$ loading on HY molecular sieve through solvothermal process, XRD did not show any information about $Cu(CH_3COO)_2 \cdot H_2O, CuCl_2 \cdot 2H_2O$ or $CuCl_2$. The result was different from Xue, and the possible reason was that the loading methods were different in adsorbent preparation. [5] Compared with the dipping method by Xue et al., the solvothermal method made the copper salts disperse on HY molecular sieve more evenly. After activation at 170 ℃, the diffraction peaks of $CuCl$ appeared, which displayed a weak diffraction peak at 28.5°, implying more $CuCl$ come into being after 170 ℃ activation [19,36]. At the same time, some $CuCl$ perhaps changed into $Cu^IY$ through ion exchange, the following TG-MS experiments confirmed this opinion. After activation at 290℃, the diffraction peaks of $CuCl$ disappeared and only a little of Cu displayed a very weak diffraction peak at 43.3°, indicating that higher activation temperature perhaps promoted the ion exchange between $CuCl$ and HY to form $Cu^IY$, the following TG-MS experiments confirmed this opinion too. Much $Cu^IY$ in adsorbent was benefit to CO adsorption, which was in agreement with the CO adsorption experiment results. At the same time, some Cu0 came into being from $CuCl$ or $Cu^{'}Y$. According to theory, experiments and literature, it was supposed that the mechanism of the copper in preparing process was below: [37-39]

$$Cu^{2+} \rightleftarrows Cu^{+} \rightleftarrows Cu \quad (2)$$

$$CuCl + HY \rightleftarrows Cu(I)Y + HCl \quad (3)$$

$$Cu^{2+} \rightleftarrows Cu^{+} \rightleftarrows Cu(I)Y \rightleftarrows Cu \quad (4)$$

It was verified that $Cu^{2+}$ and $Cu^0$ had almost no contribution to the CO adsorption of the adsorbents. Compared with $Cu^+$, $Cu^IY$ play a more important role in CO adsorption. XRD results indicated that the multiple copper valences maybe coexistence together in the adsorbents, and more explore was needed. Figure 4b illustrated the XRD patterns of HY molecular sieve and the adsorbents prepared with different amounts of copper salt. When the copper loading was 3.5 mmol $Cu^{2+}(gHY)^{-1}$, after activation at 290℃, only a little of Cu displayed a very weak diffraction peak at 43.3°. When the copper loading was 7.0 mmol $Cu^{2+}(gHY)^{-1}$, the diffraction peaks of $Cu^0$ increased at 2θ values of 43.3° and 50.4°; At the same time, the diffraction peaks of $CuCl_2$ appeared. When the copper loading was 10.5 mmol $Cu^{2+}(gHY)^{-1}$, not only the diffraction peaks of $Cu^0$ and $CuCl$ further increased, but also the diffraction peak of $CuCl_2$ appeared, indicating that copper salts overloaded on the molecular sieve. The overloaded copper salts were stacked on the molecular sieve, which had no benefit to CO adsorption. So, the optimum copper loading amount was 7.0 mmol $Cu^{2+}(gHY)^{-1}$, and the conclusion was in accord with experimental results.

### XRF Analysis

Table 3 listed the main chemical elements in the prepared adsorbents, and the mole ratio of $Cu(CH_3COO)_2 \cdot H_2O / CuCl_2 \cdot 2H_2O$ was 3. It was found that the main elements in the adsorbents were Si, Al, Cu, Cl and Na elements. With the increase of copper loading from 1.75 mmol $Cu^{2+}(gHY)^{-1}$ to 10.5 mmol $Cu^{2+}(gHY)^{-1}$, the weight concentration of copper element and chlorine element increased obviously, while the mole ratio of Cu/Cl was neither 2/1 nor 1/1. It was verified that the presence of copper on the HY molecular sieve was very complex. When the copper loading amount was 1.75 mmol $Cu^{2+}(gHY)^{-1}$, the mole ratio of Cu/Cl was 6.92, implying that the majority of the chlorine element changed into HCl via ion exchange with HY molecular sieve and evaporated from the molecular sieve, as shown in (3).

The results also indicated that, in the course of the morphological transition of copper, the molecular sieve also played a role. When the copper loading amount was 7.00 mmol $Cu^{2+}(gHY)^{-1}$, the mole ratio of Cu/Cl decreased to 2.15. Although more ion exchange occurred on the molecular sieve, it was unquestionable that more chlorine stayed on the molecular sieve. When the copper loading amount was 10.00 mmol $Cu^{2+}(gHY)^{-1}$, the mole ratio of Cu/Cl recovered a little. This may be because more Cu was generated, and Figure 4b verified this conjecture.

**Table 3:** Main chemical elements in the prepared adsorbents.

| Adsorbent | Si (Wt%) | Al (Wt%) | Cu (Wt%) | Cl (Wt%) | Na (Wt%) | Cu/Cl mole ratio | Summary (Wt%) |
|---|---|---|---|---|---|---|---|
| 1.75 mmol $Cu^{2+}$/ gHY | 61.72 | 15.01 | 17.31 | 1.39 | 1.09 | 6.92 | 96.52 |
| 3.5 mmol $Cu^{2+}$/ gHY | 43.94 | 11.58 | 33.63 | 7.28 | 0.987 | 2.52 | 97.42 |
| 7.0 mmol $Cu^{2+}$/ gHY | 30.8 | 8.52 | 45.95 | 11.59 | 0.83 | 2.15 | 97.69 |
| 10.5 mmol $Cu^{2+}$/ gHY | 25.78 | 7.31 | 51.59 | 12.29 | 0.799 | 2.29 | 97.77 |

**XPS Analysis**

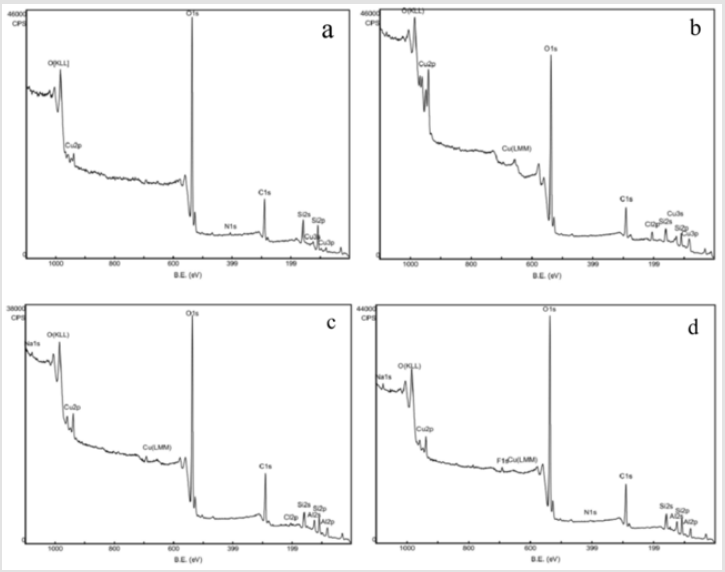


**Figure 5:** Survey XPS results of the prepared adsorbents.

In order to investigate the relationship between the valence states of the copper and the CO adsorption performance of the prepared adsorbents, XPS experiment was carried out. Figure 5a-d showed the survey XPS results of the prepared adsorbents. From Figure 5, Si, Al, Cu, Cl, C and O were all existed in the adsorbents. After activation at 170 ℃, 290 ℃ and 380 ℃, there was Si, Al, Cu, C and O still existed in survey spectra, while the characteristic peak of Cl gradually weakened and disappeared. From Figure 5, it was found that copper often existed in multiple forms simultaneously, and chlorine may be removed from the molecular sieve because of ion exchange. Figure 6 showed the XPS spectra of Cu element in the adsorbents prepared at different conditions. Before activation, the adsorbent showed two intense peaks at 935.6 eV and 954.7 eV, accompanied with the $Cu^{2+}$ satellite peak at 940-947 eV, which could be attributed to the binding energy of $Cu^{2+}$ 2p3/2 and $Cu^{2+}$ 2p1/2 respectively, as shown in Figure 6. Figure 6a also showed two intense peaks at 932.6 eV and 952.5 eV, which could be attributed to the binding energy of $Cu^{+}$ 2p3/2 and $Cu^{+}$ 2p1/2 respectively. The result was not in agreement with Gao's et.al,

and it indicated that there was $Cu^{+}$ coming into being in solvothermal process [19,40,41]. After activation at 170 °C, 290 °C and 380°C, $Cu^{2+}$ 2p3/2 peak, $Cu^{2+}$ 2p1/2 peak, $Cu^{+}$ 2p3/2 peak and $Cu^{+}$ 2p1/2 peak still existed while the height of the peaks changed, which indicated the amount of $Cu^{2+}$ and $Cu^{+}$ changed. The fitted XPS spectra of the adsorbents activated at different temperatures was listed in Figure 7. From Figure 7, it was found that the amount of $Cu^{+}$ was the highest after activation at 290 °C while the amount of $Cu^{+}$ was the lowest before activation. Combining XRD and XRF analysis, it should be emphasized that $Cu^{+}$ existed not only as $CuCl$, but more as $Cu^{I}Y$. The XPS result showed a positive correlation with the CO adsorption performance of the adsorbent, which was in agreement with the above mechanism.

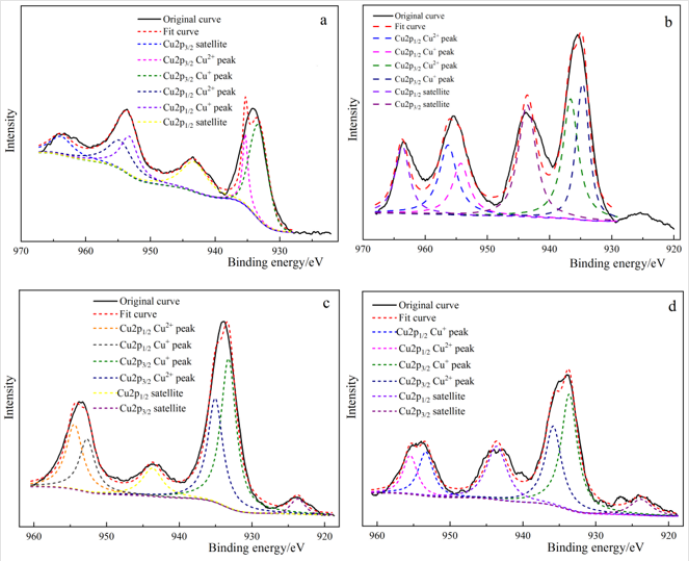


**Figure 6:** XPS spectra of adsorbents activated at different temperatures.

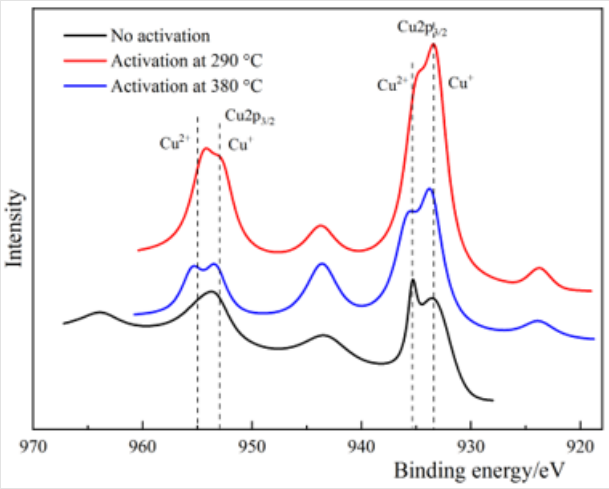


**Figure 7:** Fitted XPS spectra of adsorbents activated at different temperatures.

**TG-MS Analysis**

TG-MS experiment was conducted to investigate the mechanism of the adsorbent prepared at different stages, as shown in Figure 8. The experiment was carried out from room temperature to 290 °C at a rate of 5 °C $min^{-1}$ and then maintained for 1 h under Ar and the flow rate is 50 mL $min^{-1}$. From Figure 8a, the first step weight loss was at about 50-110 °C, which was attributed to the evaporation of water. The second weight loss step was at 150-290 °C, which was attribut-

ed to the activation of the adsorbent. In the activation process, some $Cu(CH_3COO)_2$ and $CuCl_2$ was reduced to $CuCl$, and a small amount of gases such as $H_2O$ and CO were generated correspondingly, as listed in Figure 8b. In activation process, as listed in Figure 8b too, some $CuCl$ exchanged with $HY$ molecular sieve, and a small amount of gas such as $HCl$ were generated correspondingly, as proposed in (3) [41,42].

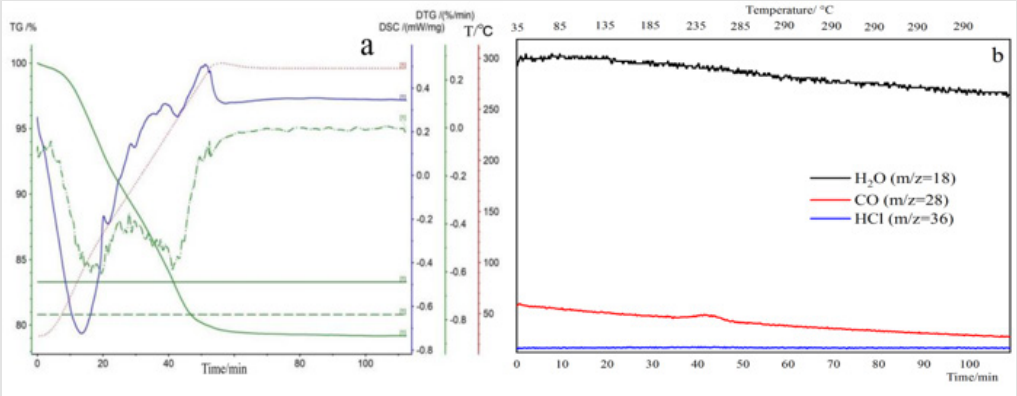


**Figure 8:** TG-MS of adsorbent preparing.

It was a pity that the mechanism was still not completely clear and further exploration were required. The question were below:

1. The role of $C_2H_5OH$ in adsorbent preparing,
2. The transform of $Cu(CH_3COO)_2$,
3. How to enhance the ion exchange in the activation process.

## Conclusion

In this paper, $C_2H_5OH$ or water was used as the dispersing agent, binary $Cu^{II}$ precursors $CuCl_2$ and $Cu(CH_3COO)_2 \cdot H_2O$ were used to prepare $Cu^{I}Y$, and the CO adsorption performance was evaluated. The conclusions were as bellow:

1. The CO adsorption breakthrough capacity prepared with $C_2H_5OH$ as dispersing agent increased by 28.4% compared to water as dispersing agent.
2. $C_2H_5OH$ played an important role in adsorbent preparation. In the preparation of the adsorbent, $C_2H_5OH$ acted as a dispersing agent, which enhanced the mass transfer and made copper salts distribute on HY molecular sieve more evenly. In addition, $C_2H_5OH$ maybe also act as a reducing agent in $Cu^{2+}$ transforming to Cu+.
3. Binary $Cu^{II}$ precursors $CuCl_2$ and $Cu(CH_3COO)_2 \cdot H_2O$ introduced more copper active sites to molecular sieve, which improved the CO adsorption capacity of the adsorbent.
4. In adsorbent preparation, copper often existed in multiple forms simultaneously.
5. Compared with $Cu^{II}$, $Cu^{0}$ and even $CuCl/HY$, $Cu^{I}Y$ played a more important role in CO adsorption. The mechanism of the adsorbent preparation was proposed in this paper, and further exploration was required.

## Acknowledgement

This work is performed by School of Chemistry and Chemical Engineering, Henan Key Laboratory of Green Coal Conversion, Distinguished Foreign Scientist Workshop on Coal Green Conversion (GZS20200012), Henan Polytechnic University for AramcoTech, under the framework of a contract of AramcoTech 2019-017/3.

## Supplementary Information Availability Notice

The authors declare no competing financial interest.

## References

1. Farshad F K N, Ehsan H, Katie D L, Tae-Sik O (2022) A highly stable CuO-derived adsorbent with dual Cu(I) sites for selective CO adsorption. Separation and Purification Technology 290: 120906.
2. Ky V, Van N L, Duong T Q, Jinsoo K (2021) Facile synthesis of spray pyrolysis-derived CuCl/γ-$Al_2O_3$ microspheres and their properties for CO adsorption and $CO/CO_2$ separation. Microporous and Mesoporous Materials 321: 111132.
3. Wu X F, Fang X, Wu L, Jackstell R, Neumann H, et al. (2014) Transition-metal-catalyzed carbonylation reactions of olefins and alkynes: a personal account. Acc Chem Res 47(4): 1041-1053.

4. Mozaffari N, Solaymani S, Achour A, Kulesza S, Bramowicz M, et al. (2020) New Insights into $SnO_2/Al_2O_3$, $Ni/Al_2O_3$, and $SnO_2/Ni/Al_2O_3$ Composite Films for CO Adsorption: Building a Bridge between Microstructures and Adsorption Properties. J Phys Chem C 124(6): 3692-3701.
5. Xue C L, Hao W M, Cheng W, P Ma J H, Li RF (2019) CO Adsorption performance of CuCl/activated carbon by simultaneous reduction¯ dispersion of mixed Cu(II) Salts. Materials 12(10): 1605.
6. Hi W, Yi B, Hou M, Z Shao (2007) The effect of $H_2S$ and CO mixtures on PEMFC performance. Int JHydrogen Energy 32(17): 4412-4417.
7. Pérez L C, Koski P, Ihonen J, Sousa J M, Mendes A J (2014) Effect of fuel utilization on the carbon monoxide poisoning dynamics of Polymer Electrolyte Membrane Fuel Cells. Power Sources 258(15): 122-128.
8. Zarca G, Ortiz I, Urtiaga A (2013) Copper(I)-containing supported ionic liquid membranes for carbon monoxide/nitrogen separation. J Membr Sci 438: 38-45.
9. William G, Iise E (1930) Ind Eng Chem 22(4): 382.
10. Patil G S, Baruah S, Dutta N N (1991) Gas Sep 5: 2.
11. Tsutaya H, Izumi J (1991) Zeolites. 11: 90.
12. Grande C A, Lopes F V S, Ribeiro A M, Loureiro J M, Rodrigues A E (2008) adsorption of off-gases from steam methane reforming ($H_2$, $CO_2$, $CH_4$, CO and $N_2$) on Activated Carbon. Sep Sci Technol 43(6): 1338-1364.
13. Hirai H, Komiyama M, Hara S (1982) Makroml Rapid Comun 3: 95.
14. Yin Y, Wen Z, Shi L, Zhang Z, Yang Z, et al. (2019) Cuprous/vanadium sites on MIL-101 for selective CO adsorption from gas mixtures with superior stability. ACS Sustain Chem Eng 7: 11284-11292.
15. Mishra P, Mekala S, Dreisbach F, Mandal B, Gumma S (2012) Adsorption of $CO_2$, CO, $CH_4$ and $N_2$ on a zinc-based metal organic framework. Sep Purif Technol 94: 124-130.
16. Unger K (1972) Structure of porous adsorbents, Angew. Chem Int Ed Engl 11: 267.
17. Liu W, Pan X M, Wang J, Zhao B Y, Xie Y C (2001) Acta Chimica Sinica 59: 1021.
18. Xue C L, Hao W M, Cheng W P, Ma J H, Li R F (2019) Effects of pore size distribution of activated carbon (AC) on CuCl dispersion and CO adsorption for CuCl/AC adsorbent. Chemical Engineering Journal 375: 122049.
19. Gao F, Wang Y Q, Wang S H (2016) Selective adsorption of CO on CuCl/Y adsorbent prepared using $CuCl_2$ as precursor: Equilibrium and thermodynamics. Chemical Engineering Journal 290: 418427.
20. Rabo J A, Francis J N, Angel C L (1977) US 4019879 [P] 04: 26.
21. Xie Y C, Zhang J P, Tong X Z (1997) Journal of Chemistry 18(7): 1159.
22. Takahashi A, Yang R T, Munson C L (2001) Cu(I)–Y-Zeolite as a superior adsorbent for diene/olefin separation. Langmuir 17(26): 8405-8413.
23. Sun S, Wu Y Y, Luo S Z (201l) Journal of Chemistry of Higher Learning 8: 1794.
24. He G, Sun L, Song X (2011) Energy & Fuels 25(8): 3506.
25. Golden T C, Kratz W C, Wilhelm F C (1992) US Patent 6: 30.
26. Hirai H, Wakabayashi H, M K (1986) Bulletin of the Chemical Society of Japan 59(2): 367.
27. Zhang Z B (2021) Dalian University of Technology. p. 5.
28. Li Z, Wang R Y, Zheng H Y, Xie K C (2010) Preparation of $Cu^IY$ catalyst using $CuCl_2$ as precursor for vapor phase oxidative carbonylation of methanol to dimethyl carbonate. Fuel 89(7): 1339-1343.
29. Helen H Y, Padin J, Yang R T (1999) Ind Eng Chem Res 38: 2720.
30. Peng J, Xian S, Xiao J, Huang Y, Xia Q, et al. (2015) A supported Cu(I)@MIL-100(Fe) adsorbent with high CO adsorption capacity and $CO/N_2$ selectivity. Chem Eng J 270: 282-289.
31. Kanghee C, Jungsu K, Jong-ho P, T Jung, Hee T B, et al. (2019) High CO adsorption capacity, and CO selectivity to $CO_2$, $N_2$, $H_2$, and $CH_4$ of CuCl/bayerite adsorbent. Microporous Mesoporous Mater 277: 142-148.
32. Yin A, Guo X, Dai W, Fan K (2009) The nature of active copper species in Cu-HMS catalyst for hydrogenation of dimethyl oxalate to ethylene glycol: New Insights on the Synergetic Effect between $Cu^0$ and $Cu^+$. J. Phys. Chem. C 113: 11003-11013.
33. Yang S I, Choi D Y, Jang S C, Kim S H, Choi D K (2008) Hydrogen separation by multi-bed pressure swing adsorption of synthesis gas. Adsorption 14: 583-590.
34. Bloch E D, Hudson M R, Mason J A, Chavan S, Crocella V, et al. (2014) Reversible CO binding enables tunable $CO/H_2$ and $CO/N_2$ separations in metal–organic frameworks with exposed divalent metal cations. J Am Chem Soc 136: 10752-10761.
35. Zhang J L, Li D P, Weng Y J, Sun Q, Duval S A, et al. (2023) Performance assessment of molecular sieves for sulfur recovery unit tail gas treating. I & EC Research 62: 1499-1507.
36. Nam J K, Choi M J, Cho D H, Suh J K, Kim S B (2013) The influence of support in the synthesis of dimethyl carbonate by Cu-based catalysts. J Mol Catal A: Chem 370: 7-13.
37. Iwamoto M, Hamada H (1991) Catalysis Today 10(1): 57.
38. Qin J X, Wang Z M, Liu X Q, Y X Li, L B Sun (2015) Low-temperature fabrication of Cu(i) sites in zeolites by using a vapor-induced reduction strategy. Journal of Materials Chemistry A 3(23): 12247.
39. Dorothée B, Gérard D (2006) Recent Advances in $Cu^I$/IIY: Experiments and Modeling. Catalysis Reviews 48(3): 269313.
40. Ahmed I, Jhung S H (2015) Remarkable improvement in adsorptive denitrogenation of model fossil fuels with CuCl/activated carbon, prepared under ambient condition. Chem Eng J 279: 327-334.
41. Xue C L (2019) Taiyuan university of technology 6.
42. Wei J T, Liu X, Guo Q H, Chen X L, Yu G S (2018) A comparative study on pyrolysis reactivity and gas release characteristics of biomass and coal using TG-MS analysis. Energy Sources A Recovery Util Environ Eff 40(17): 2063-2069.

**ISSN: 2574-1241**

DOI: 10.26717/BJSTR.2023.53.008474

Jiali Zhang and Yulong Zhang. Biomed J Sci & Tech Res



**Submission Link**: https://biomedres.us/submit-manuscript.php